Advances in Phytochemistry, Textile and Renewable Energy Research for Industrial Growth – Nzila et al. (Eds)

Mitigation of power outages in Rwanda

Boniface Ntambara & Paul M. Wambua
Department of Manufacturing, Industrial and Textile Engineering, School of Engineering, Moi University, Eldoret, Kenya

S. Simiyu Sitati
Department of Electrical and Communication Engineering, School of Engineering, Moi University, Eldoret, Kenya

Jean B. Byiringiro
Siemens Mechatronics Certification Center, Dedan Kimathi University of Technology, Nyeri, Kenya

ABSTRACT: Power outages in Rwanda severely affected most of the Western and Northern grids of Rwanda in 2018, 2019, and 2020. This paper studied the causes and mechanism of power outages and developed the methods and techniques to mitigate the power outages. Two operational elucidations such as a balanced steady state control system and an optimal overcurrent relay settings model for operational HV substation relay coordination have been proposed and developed. The sustainable synchronism between Rwanda Power system regions was becoming difficult over time due to load disturbances/changes. The under and over frequency, and under and over voltage load shedding techniques have been taken to reduce and mitigate the system outages. However, in order to minimize power outages in emergency regions, these systems have been extended in different regions such as Western and Northern grids which need to be maintained. The PID controllers for enhancing and mitigating the power outages have been developed in single and two area power systems. The load disturbance injection of 50MW has been created. Matlab/Simulink 2017a have been used to simulate the frequency load control, overcurrent relay, and power system models. The relay coordination and settings for a 110/15kV substation with a 17156.48A and 13987.10A of maximum and minimum fault currents, plug setting (PS), and actual operating time of the different relay have been ascertained and modeled. The simulation results have been compared with and without PID controller installation in the power system and it has been shown that the frequency response characteristics for single and two area networks in western and northern grids have been minimized to 0.0 Hz, 0.0 Hz, and 2.5 sec for overshoots, steady state errors, and settling times after cascade outages respectively. The overcurrent substation relays have been coordinated with the expected times of 0.0924–0.0622sec, 0.0949–0.0720 sec, and 0.0764–0.0661sec for extremely, very, and standard inverse relay characteristics, respectively.

Keywords: Overcurrent relay; Frequency Load Control; Power Outages; Matlab/Simulink 2017a; PID controllers; power system stability.

1 INTRODUCTION

The power outages in Rwanda clearly demonstrated the relevance of the severe problems of loss of supply and MW loss. The situation is further complicated by the necessity for the power system to survive under competition and uncertain conditions. Based on a detailed power outage analysis, the dangerous overload of the transmission grid is held as a key element initiating the development of many cascading processes (Zalostiba 2020). The outages which occurred in Rwanda from 2018 to June 2020, have mostly proven severe and very significant. It has been reported that during the power outages, about 5 million people have been affected in 5 districts from the Northern region and 5 districts from the Western region, and 70 MW of loads were lost, which is about 27% of the total load. Some other major outages began when lightning and overloading caused the tripping of a major transmission line between Western and Northern grids. Research work in these two regions are aimed at predicting voltage collapse and voltage overload with a view to controlling and reducing its occurrence on power system networks (Weiss 2019).Most of power outages are triggered by distribution circuit failure (Wang L. 2016). Conventionally overcurrent relay settings are provided based on the full load current of power system components. Load frequency control was based on many power control advanced concepts and the dynamic behavior of many industrial plants is heavily influenced

DOI 10.1201/9781003221968-7

by disturbances and in particular, by changes in the operating point (M. Wadi, 2017). The problem of coordinating protective relays in power system networks consists of selecting their suitable settings such that their fundamental protective function is met under the requirements of sensitivity, selectivity, reliability, and speed. In a modern power system, abnormal conditions can frequently occur to cause interruption to the supply, and may damage the equipment connected to the power system, which allows us to note the importance of designing a reliable protective system (Mancer N, 2015). The power system is the interconnection of more than one control areas through tie lines. The generators in a control area always vary their speed together (speed up or slow down) for the maintenance of the frequency and relative power angles to the predefined values in both static and dynamic conditions. If any sudden load change occurs in a control area of the interconnected power system then there will be frequency deviation as well as tie line power deviation (Behera, 2019). The cascade outages that occurred in Rwanda from 2018 to 2020 mostly proved severe and very significant. It has been reported that during the power outages about 5 million people have been affected in 5 districts from the Northern region and 7 districts from the Western region, and 70 MW of load were lost, which was about 27% of the total load. Some other major cascade events began when lightning and overloading caused the tripping of a major transmission line between the Western and Northern grids. Research work in these two regions aimed to predict voltage collapse and voltage overload with a view to controlling and reducing its occurrence on power system networks (Weiss R. 2020). Electrical energy is a primary prerequisite for economic growth. The demand for electrical energy has greatly increased due to large-scale industrialization. A modern power system operates under stressed conditions because of the growth in demand and the deregulation of electric power system. This leads to many problems associated with the operation and control of power systems. The economics of power generation has been a major concern for the power utilities (P. K. Modi, 2006). Power systems are becoming heavily stressed due to the increased loading of the transmission lines and due to the difficulty of constructing new transmission systems as well as the difficulty of building new generating plants near the load centers. All of these problems lead to the voltage stability problem in the power system (Z. Osman, 2006). The effective power system in Rwanda relies heavily on the ability of engineers to ensure a continuous and reliable service in cascade outages. In the ideal case, the load feeding should be at a constant frequency of 50 Hz and voltage. For reasonable operation of consumer devices, voltage and frequency should be maintained and secured within tolerable limits in practical applications. A voltage decrease from 10% to 15% or a reduction in frequency of system can cause stalling of the device loads (Tanwani, 2013). The first requirement of this is the maintenance of parallel operation of the synchronous generator with the necessary ability to grip the load condition. Because, if synchronism between the generator and the systems is missing at any time, it will affect the voltage and current instability and system relays will disconnect the supply at faulty sections (Naresh K. Tanwani, 2014). The load frequency control problems are denoted by regulating the active power output to generate units responding to the disturbances in system frequency and load power interchanges within the prescribed ranges (Congzhi Huang, 2017). The secure operation of power systems with the variation of loads has been a challenge for power system engineers since the 1920s. (Steinmetz, 1920). The voltage and frequency instability in the short term is driven by fast recovering load components that tend to restore power consumption in the time frame of seconds after a voltage drop caused by a contingency. The PID controller and Automatic Voltage Regulator have been shown to be more effective for the enhancement and optimization of power system stability with better damping under small and large disturbances when compared with conventional excitation control (M. J. Hossain, 2009).

2 MATERIAL AND METHODS

2.1 *Balanced state control system*

In this research, the PID controllers for frequency load control have been employed. The parameters and setting values of single and two area generation of hydroelectric power plants like the rated power load of 200 MW, load disturbance of 50 MW, turbine time constant of 0.5 sec, governor time constant of 0.2 sec, generator inertia constant of 5 sec, governor speed regulation of 0.05 p.u, power system time constant of 10 sec, and motor load damping coefficient of 0.6 p.u have been chosen and employed into Ntaruka and Nyabarongo Hydroelectric power plants as shown in Figures 2, 3, 5, and 6 in the Northern and Western grids, which have been controlled at Gikondo National Network Dispatching and Control. The Northern electricity grid has been monitored to check whether there were any cascade blackouts or changing conditions during the system normal operation. The system condition was evaluated by computing the frequency load system using PID controllers. These control schemes have checked the frequency deviation and drips, demand–supply power imbalance, and load change to ensure the reliability and stability of the power system. When the system was determined to be secure (not vulnerable), the monitoring system has continued in operating condition. Otherwise, the vulnerable parts and conditions were identified. As the possible unbalanced frequency and overload problems for those vulnerable conditions have occurred, they were predicted, and suitable and corresponding control strategies to mitigate and prevent the power blackouts were identified and activated whenever needed. The models and simulations of the scenarios have been computed using

Matlab 2017a/Simulink. Figure 1 demonstrates the flowchart of power cascade outages detection and the load–supply power imbalance control from the start of monitoring of the power system to the provided frequency control mechanism.

The governor regulated the turbine speed, load-supply power and the grid frequency by starting the turbine from a still condition and varied the load on the turbo-generator in imbalance conditions. The 0.8% load variation caused 1% frequency change. The rated load active power of 200 MW, nominal frequency of 50 Hz, and a sudden load disturbance of 50 MW have occurred in both area power systems, as shown in Figures 2 and 5 for no PID installed and Figures 3 and 6 for PID installed. The single area power systems without and with PID controllers have been computed and modeled as shown in Figures 2 and 3. The two area power system has been considered in unbalanced frequency load control and the generators have been interconnected in series with the loads fed, and the load disturbances have been applied in area 1 and the two power generations have been synchronized as indicated in the Figures 5 and 6. Figures 4 and 7 show the setting values and parameters of PID controllers in a single area, area 1 and area 2 in two area power generations, respectively. The performance characteristics of power and frequency in two area power generations with and without PID controllers have been observed, recorded and plotted in Figures 10, 13–16.

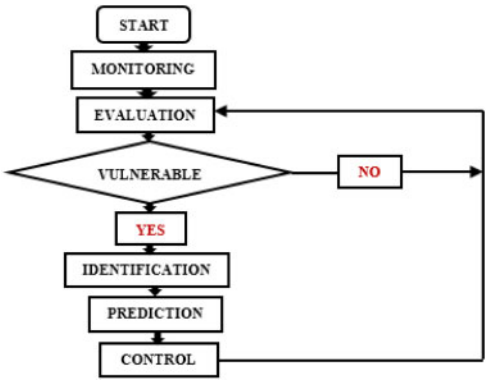

Figure 1. Flowchart of detection for cascade outages minimization in power balance steady system.

2.2 *Optimal overcurrent relay settings for effective substation relay coordination*

The values and parameters of grid and feeder impedance equivalences, phase to phase fault currents, current settings of 110 kV incomer and 15 kV outgoing feeders, and operating times for relay characteristics of the studied Rwanda power system have

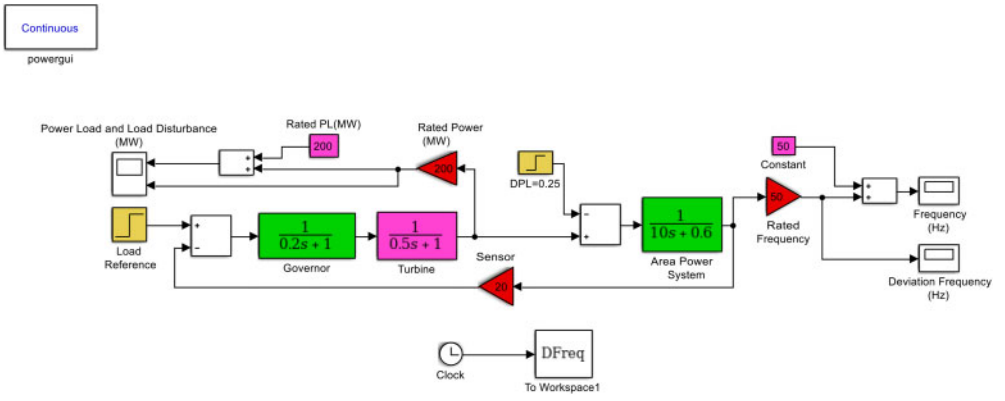

Figure 2. Rwanda Northern grid at Ntaruka hydropower plant without PID controller.

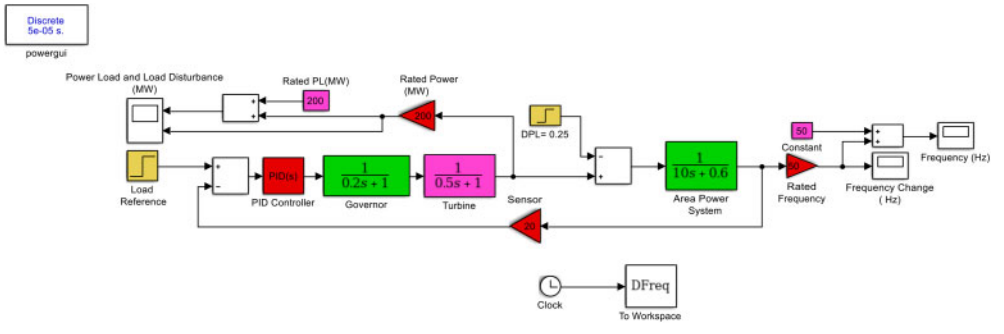

Figure 3. Rwanda Northern electricity grid at Ntaruka hydropower plant with PID controller.

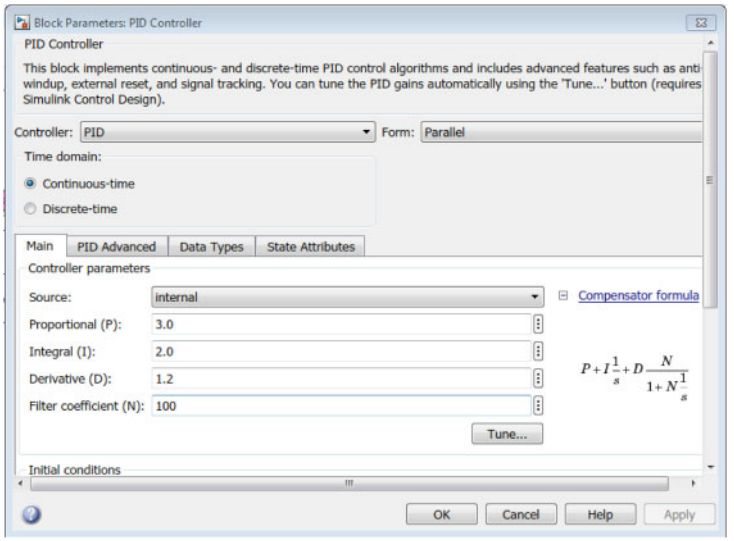

Figure 4. PID setting values of proportional, integral, and derivative.

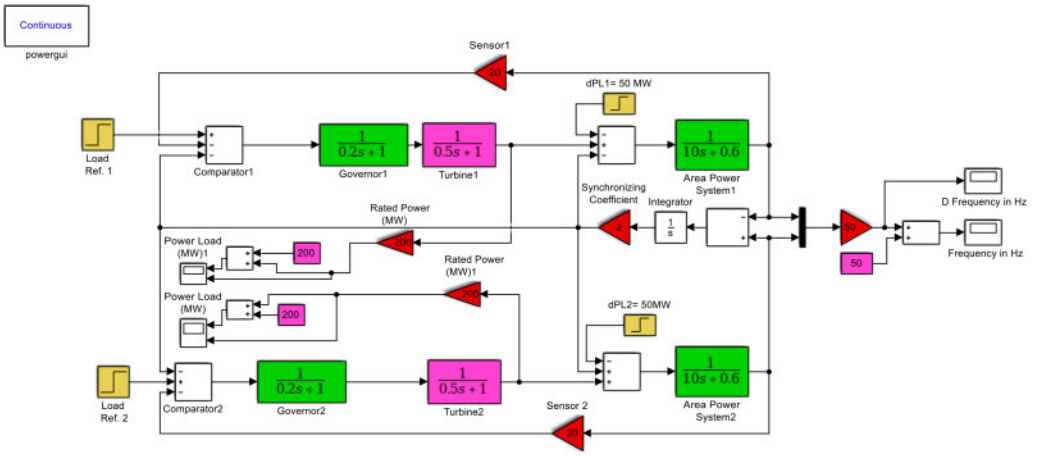

Figure 5. Two area networks without PID controllers.

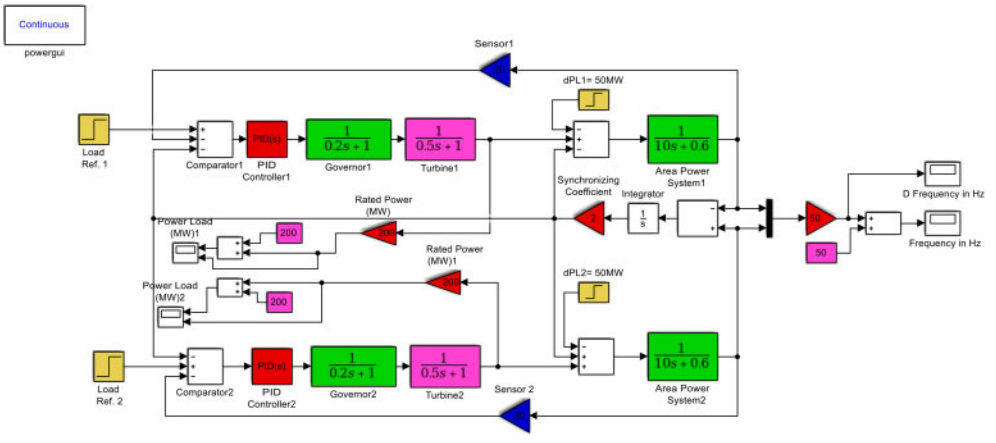

Figure 6. Two area PID controllers of the two area power generation.

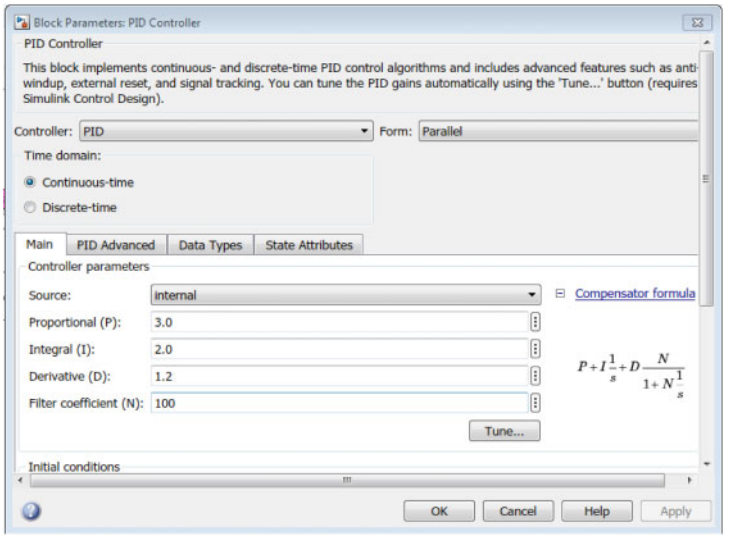

Figure 7. PID controller settings in area 1 and area 2.

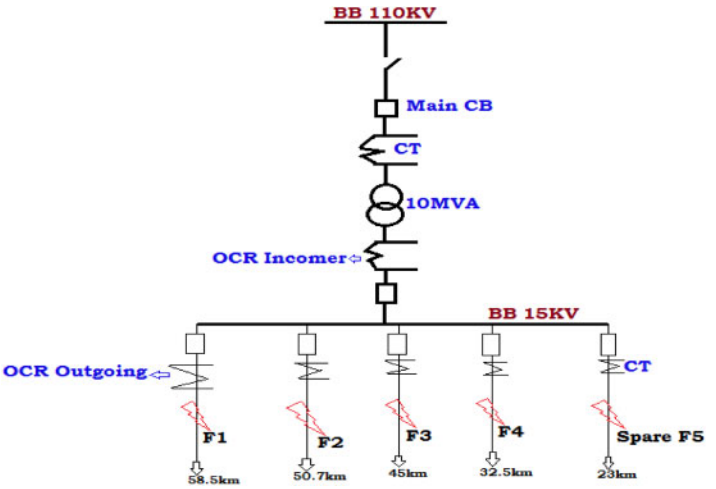

Figure 8. Incoming and outgoing (feeders) for overcurrent relay coordination and protection.

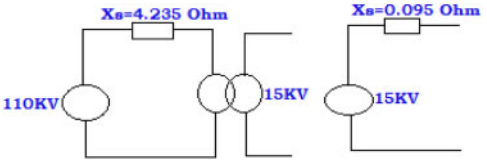

Figure 9. Reference of Xs from BB 15 kV.

been calculated and determined. The maximum and minimum fault currents from the last 3 years were recorded and documented. Figure 12 demonstrates a single line schematic of a substation with transformer 110/15 kV, 10 MVA, distributed feeders F1, F2, F3, F4, and spare F5 considering fault locations. The network MVA short circuit is 2587 MVAsc, both positive and negative sequence impedance of feeder $(Z_1 = Z_2)$ is$0.045 + j0.151\Omega$/km. The power system parameters like (X/R ratio = 5, CT ratio = 2500/4A, line length = 100 Km, positive and zero sequence resistances = 0.04553 and 0.1517Ω/km respectively, positive and zero sequence inductances = 0.000617 and $0.001533H$/km respectively full load current = 1840.9A, line capacity = 282 MVA, TMS = 0.05, line voltage = 110 kV and CT ratio for outgoing feeders = 500/1A, grid frequency = 50 Hz and real power = 70 MW have been considered and collected from Rwanda Energy Group Ltd under the Energy Utility Corporation Limited subsidiary and introduced into the power system grid to simulate the results from the power system Matlab model (see Figure 10). From the simulation of relay status as indicated in Figure 11, the performance of these relays has been achieved in a reliable and sensitive way and Figure 12 shows how voltages

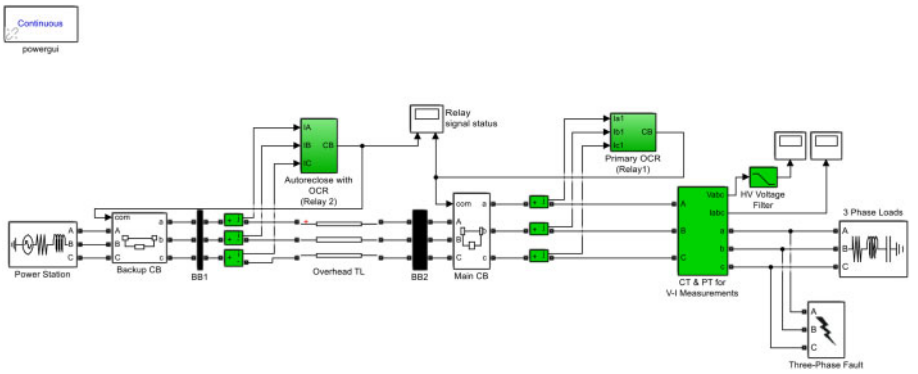

Figure 10. Power system grid with occurred faults model.

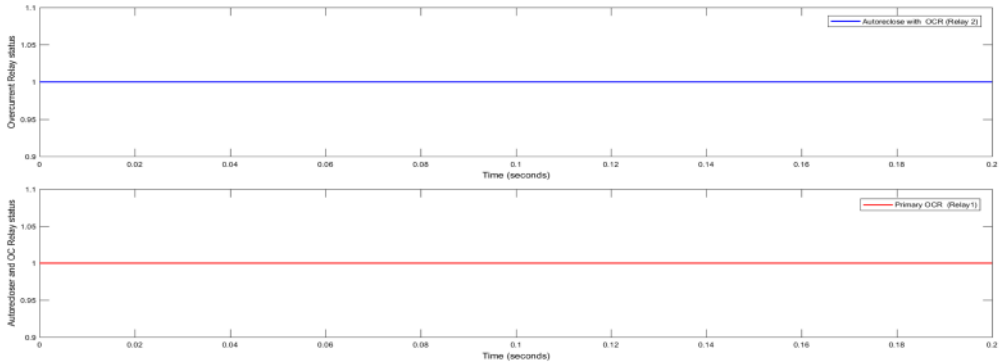

Figure 11. Power network relay status for good operational state.

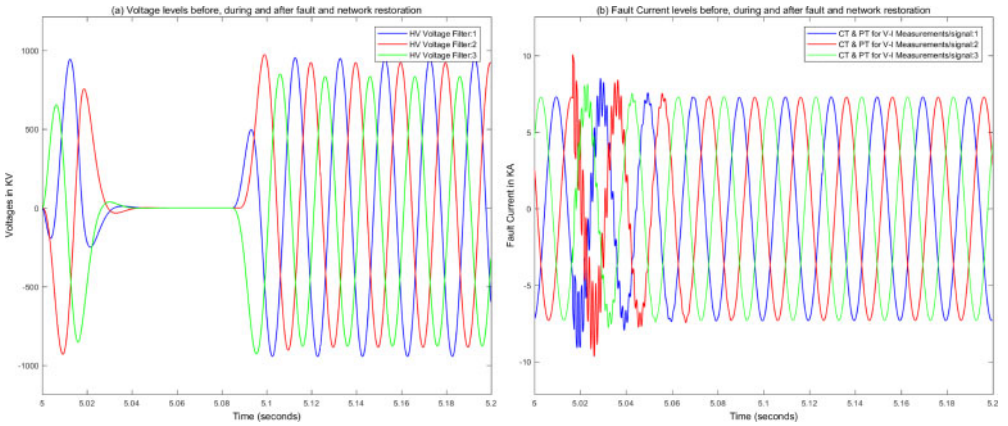

Figure 12. (a) Voltages and (b) fault currents observed during simulation on the power system.

and currents behaved before, during, and after power outages along the network. The relay characteristics in terms of operating times, as shown in Table 5, have been observed during simulation.

2.2.1 *Phase fault currents determination*

The calculation of phase short circuit currents requires the data of grid impedance (X_{s110KV}), transformer impedance (X_t) and feeder impedance (X_f) at fault location.

The impedance of feeder line varied with the feeder distance; the length in consideration was from the 15 kV bus bar to the outgoing feeder fault location. The outgoing of the five feeders, F1 was selected for the purpose of illustration for the short circuit current calculations, since the longest (58.5 km) has

Table 1. Feeder impedance calculation.

% Length	Feeder Impedances
0	0
1	1%*58.5*(0.045 + j0.151)= 0.026+j0.088

been considered. Table 1 shows the calculation of the feeder impedance at a distance of 0% (bus bar 15 kV) and 1% of the length of the F1 feeder. Let $Z_1 = Z_2 = 0.045 + \text{j}0.151$.

The grid impedance 110 kV

$$X_{S110KV} = {(KV)^2}/{\text{MVAsc}} = {(110)^2}/{2587} = 4.2352\Omega \quad (1)$$

The grid impedance 15 kV,

$$X_{S15KV} = \frac{(X_{S15KV})^2}{(X_{S110KV})^2} \times (X_{S110KV}) = \frac{15^2}{110^2} \times 4.2352 = 0.095\Omega \quad (2)$$

Transformer impedance

$$(X_t) = \frac{(kV)^2}{MVA} \times 8.67\% = \frac{(15)^2}{10} \times 8.67\% = 1.95\Omega \quad (3)$$

The reduced equivalence impedance diagram is shown in Figure 9.

The equivalent of impedance in the fault location was calculated in series,

$$Z_{1eq} = Z_{2eq} = X_{s(15KV)} + X_t + X_{F1} = 0.045 + j0.151 + X_{F1}X_{F1} = j0.095 + j1.95 = j2.045 \quad (4)$$

Table 2 indicates the feeder impedance equivalence of fault positions 0% and 1% respectively.

Table 2. Feeder impedance equivalence calculation.

% Length	Feeder Impedances
0	j2.045
1	$j2.045 + 0.026 + j0.088 = 0.026 + j2.133$

Phase to phase short circuit current (I_{SC}) in the feeder is affected by positive and negative sequence of equivalent impedance (Z_{1eq} and Z_{2eq}) at fault location.

$$I_{SC} = \frac{V}{Z1eq + Z_{2eq}} = \frac{V}{2Z_{2eq}} \quad (5)$$

where V is ph–ph voltage. Based on equations (5) and Table 1 for equivalent of impedances following the 25%, 50%, 75%, and 100% feeder locations, by imitating the same procedures, the short circuit currents found after calculation are tabulated in Table 3.

Table 3. Calculated and protected fault current levels based on maximum fault occurrences.

% Length	Calculated Fault level Current (A)	Occurred Fault Level (A)	Protected Fault Current Level (A)
0	3667.48	13489($I_{fault-max}$)	17156.48
1	3515.92		17004.92
25	1833.96		15322.96
50	985.02		14474.02
75	655.76		14144.76
100	498.10	1617($I_{fault-min}$)	13987.10

The current setting (I_{set}) of the OCR relay is 120% of the full load (I_n) equipment installed. The lowest current installed transformation is 1840.9 A. Selected 120% × I_n must be planned for extreme load forbearance.

$$\text{I}_{\text{set}} = 120\% \times I_{\text{n}} = 120\% \times 1840.9 = 2209.08 \text{ A}. \quad (6)$$

The outgoing feeder utilized a current transformer ratio of 500 / 1 A. The setting current (I_{set}) of the OC relay is 120% of the full load current ($I_{full-load}$) of the installed equipments (CT) 500 A.

$$\text{I}_{\text{set}} = 120\% \times I_{\text{full-load}} = 120\% \times 500 = 600\text{A} \quad (7)$$

2.2.2 *Calculation of operating time of OCR (t_{OCR})*

The time multiplier setting (TMS) and working time (t_{OCR}) based on the short circuit current on 15 kV bus have been regulated to 0.05 and calculated respectively.

$$\text{SIR (t)} = \frac{0.14}{\text{Psm}^{0.02} - 1} \times \text{TMS}, \quad (8)$$

$$\text{IR (t)} = \frac{13.5}{\text{Psm} - 1} \times \text{TMS} \quad (9)$$

$$\text{EIR (t)} = \frac{80}{\text{Psm}^2 - 1} \times \text{TMS} \quad (10)$$

where

$$\text{Psm} = \frac{\text{I}_{\text{SC}}}{\text{I}_{\text{set}}}. \quad (11)$$

By replacing (11) in (8), (9), and (10) we get: standard inverse relay, $\text{TMS} = \frac{\left(\frac{\text{I}_{\text{sc}}}{\text{I}_{\text{set}}}\right)^{0.02} - 1}{0.14} \times \text{t}_{\text{OCR}}$, t_{OCR} is OCR tripping time when fault occur at 15 kV bus bars;

$$\text{t}_{\text{OCR}} = \frac{0.14}{\left(\frac{\text{I}_{\text{sc}}}{\text{I}_{\text{set}}}\right)^{0.02} - 1} \times \text{TMS}; \quad (12)$$

very inverse relay,

$$\text{TMS} = \frac{\left(\frac{I_{sc}}{I_{set}}\right) - 1}{13.5} \times t_{OCR},$$
$$t_{OCR} = \frac{13.5}{\left(\frac{I_{sc}}{I_{set}}\right) - 1} \times \text{TMS}; \quad (13)$$

extremely inverse relay,

$$\text{TMS} = \frac{\left(\frac{I_{sc}}{I_{set}}\right)^2 - 1}{80} \times t_{OCR},$$
$$t_{OCR} = \frac{80}{\left(\frac{I_{sc}}{I_{set}}\right)^2 - 1} \times \text{TMS}; \quad (14)$$

t_{OCR} is tripping time of overcurrent relay Figure 10 demonstrates the power system model to be set and coordinated using overcurrent relays

3 RESULTS AND DISCUSSIONS

3.1 *Frequency response characteristics*

In this research paper, during the load disturbance conditions, frequency load PID controllers have been developed and performed in balancing steady state condition by considering the values of overshoot, steady state error, and settling time. The frequency has been stabilized and balanced by using PID controllers in single area and two area hydroelectric power plants. The simulation results in Table 4 and in Figures 13–16 for single and two area power systems show that by applying a step load increment of 0.25 p.u MW equivalent to 50 MW before PID controller installation, the generation plants have been collapsed with an overshoot of 0.02 Hz, a steady state error of 0.55 Hz, and a settling time of 10 sec. After PID controller installation in the generation control station and National Dispatching, the power system was recovered to normal state at 0.0 Hz, 0.0 Hz, and 2.0 sec for overshoot, steady state error, and settling time, respectively (see Figure 14 and 16). The generation power plants have been synchronized with a synchronization parameter as shown in Figures 5 and 6, and the simulation results show that by setting the PID controller and install in a power network, the overshoot, steady state error, and settling time have been minimized to 0.0 Hz, 0.0 Hz, and 2.5 sec, respectively, and it has been observed that the frequency has been recovered and remained at 50Hz after load disturbance. Table 2 shows the summarized simulation results of single and two area power systems of the frequency responses before and after PID application in the hydropower station.

Summarizes the single and two area power system frequency results before and after plant perturbations.

Table 4. Simulation results of frequency response.

SINGLE AREA			TWO AREA	
Frequency Response Characteristics			Frequency Response Characteristics	
Before PID		After PID	Before PID	After PID
Overshoot (Hz)	**0.02**	**0**	**0.03**	**0**
Settling time (Sec)	**10**	**2.5**	**10**	**2.5**
Steady state error (Hz)	**0.55**	**0**	**0.57**	**0**
Recorded nominal frequency (Hz)	< 49.5	**50**	< 49.5	**50**

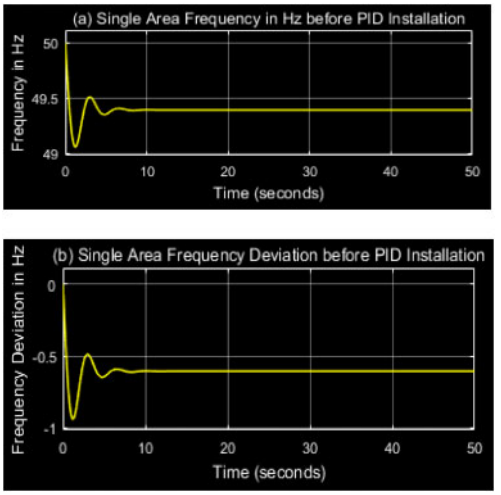

Figure 13. Frequency response without PID controller with load disturbance injection.

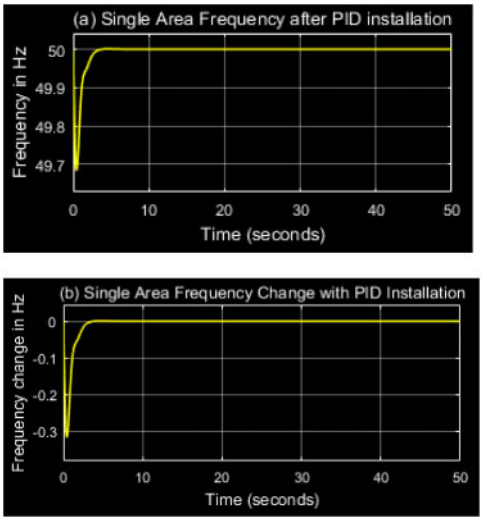

Figure 14. Frequency response with PID controller with load disturbance injection.

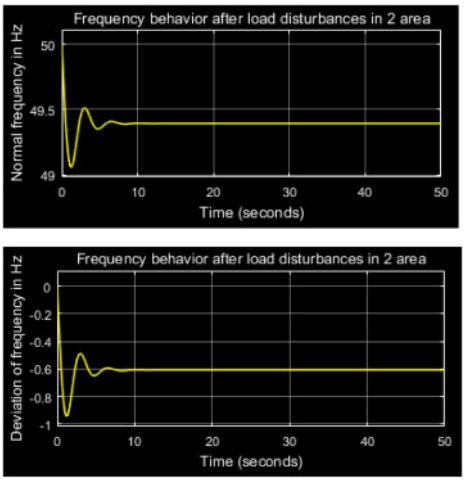

Figure 15. Frequency response of two area power generation without PID controllers.

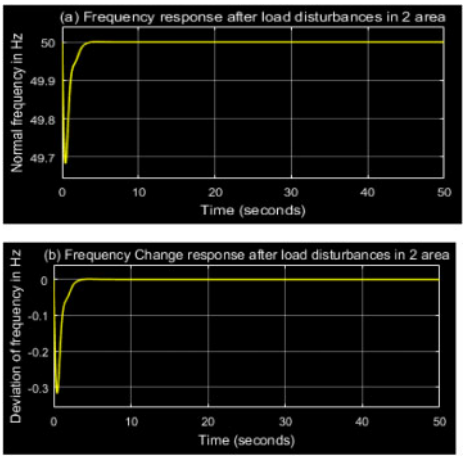

Figure 16. Synchronized frequency response with PID controllers in two areas after disturbances.

3.2 *Overcurrent setting and substation relay coordination*

Results summarized in Table 5 and Figure 17 are based on Table 5 with equations (5), (6), (7), (8), (9), (10), (11), (12), (13), and (14). Calculations were made of operating times of overcurrent relay incoming and outgoing for SIR, VIR, and EIR using I_{set} and I_{SC}.

Table 5. Operating time of incoming and outgoing feeders of OCR characteristics.

Fault Positions (%)	Operating Time (t_{OCR}) in secs					
	OCR INCOMING			OCR OUTGOING FEEDERS		
	EI	VI	SI	EI	VI	SI
0 (15 kV BB)	0.067	0.099	0.167	0.0048	0.0244	0.1009
1	0.068	0.111	0.168	0.0049	0.0246	0.1011
25	0.084	0.113	0.177	0.0061	0.0275	0.1045
50	0.095	0.121	0.182	0.0068	0.0291	0.1064
75	0.100	0.124	0.185	0.0072	0.0299	0.1072
100	0.102	0.126	0.186	0.0073	0.0302	0.1076

Relay coordination and settings were generally based on their characteristics, which indicated the speed of operation. The characteristics are: Standard Inverse (SI), Very Inverse (VI), and Extremely Inverse (EI). From Figure 17 and Table 5, it was observed that the extremely inverse, very inverse, and standard inverse were working at 0.067–0.102 sec, 0.099–0.126 sec, 0.167–0.186 sec, and 0.0048–0.0244 sec, 0.1009–0.0073 sec, 0.0302–0.1076 sec for overcurrent incoming and outgoing feeders, respectively. The operating time of overcurrent incoming and outgoing feeders were calculated based on the short circuit currents demonstrated in Table 3, and for a time setting multiplier that was set at 0.05 sec (IEC standards), and

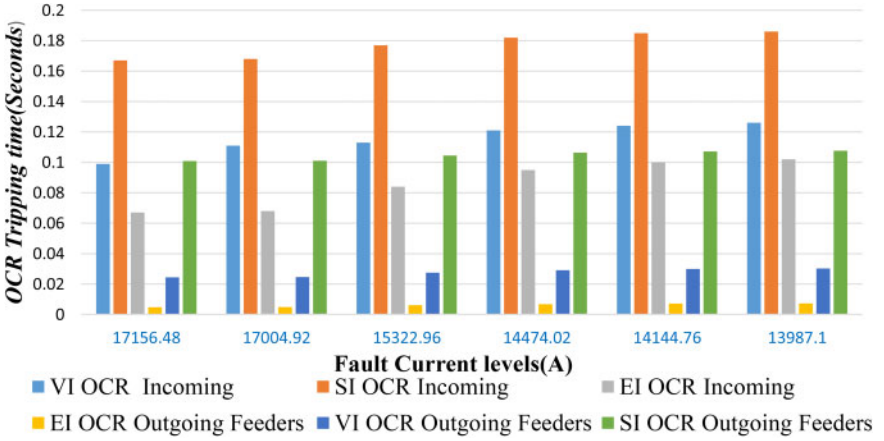

Figure 17. Operating times of overcurrent relay incoming and outgoing feeders.

also based on equations (5), (6), and (7). By application of autorecloser and overcurrent relays and creation of three phase faults in the power network, it has been shown that there was improvement and optimization of voltages and currents waveforms in the transmission line before, during, and after fault occurrences and the outages were cleared (see Figure 12). As the power outages occurred as shown in Figure 10, Relay 1 and Relay 2 were coordinated and sent the tripping signals to Backup CB and Main CB1, respectively, to open and isolate the power system grid and trip the network; the currents increased rapidly, waited for fault clearance restoration signals from relays, and restored quickly. The voltages decreased to zero volts instantly, as shown also in Figure 12. This meant that during the outages, overcurrent and autorecloser relays for extremely inverse tripped at a very short time, as indicated in the Table 5 and Figure 17 normally. Whenever a transient fault has occurred in the system, the autorecloser relay checked the synchronism of the network and the outages were mitigated and prevented. From voltage parts, at the 5^{th} sec, the grid worked normally, after 0.02 sec, an outage occurred, was recorded, and remained in the power system for a period of 0.064 secs, after which the autorecloser with an overcurrent relay commanded the main CB to trip and isolated the faulted part within 0.064 sec; at 5.084 sec it became normal, protected, and optimized. Like the fault current's part, at 5 sec, the system normally worked within 0.01 sec, when the network was faulted during 0.04 secs and restored at 5.05 secs. With reference to Figure 17 and Table 5, the time of operation of overcurrent relays varied, with the extremely inverse relay the smallest, followed by the very inverse and standard inverse for both overcurrent relay incoming and outgoing feeders, respectively. It should be also observed that the three relay characteristics have been considered during the relay settings. The standard inverse characteristic took care of faults within the utility substation. The very inverse characteristic took care of faults at the midpoint of the feeder, while the extremely inverse characteristic took care of faults at the far end of the feeders.

4 CONCLUSIONS AND RECOMMENDATIONS

In this paper, we presented a frequency-based load control scheme to balance demand with supply and regulated frequency in a power system. We set up a load control optimization problem with the objective of minimizing the total frequency variation/error and the constraint of demand–supply power balance. The load frequency PID controllers using local frequency measurements per unit to solve the load disturbances and prove the convergence of the controllers have been designed. Numerical experiments have demonstrated that the proposed PID load control scheme was able to relatively quickly balance the power demand with supply and restore frequency under generation-loss. It can be observed that under steady state condition, incremental turbine power output of single and two area in which disturbance were given, became equal to the load disturbance and that of other area became zero along with zero tie-line power deviation with the controllers used in frequency load control of the case studies. Further research should deal with more than two frequency control areas in a microgrid to ensure the reliability and the security of the generation, transmission, and distribution systems. The overcurrent relay characteristics were developed and modeled in MATLAB/SIMULINK. The performance characteristics of the overcurrent relay were evaluated at a location with three-phase faults. The protection of a 110/15 kV substation with two bus systems and its relay settings has been presented. The optimal coordination of overcurrent with extremely inverse time is better than very inverse and standard inverse characteristics because overcurrent relay feeders as the main protection and overcurrent incoming as backup protection were able to work faster to protect the distribution system from phase-to-phase short circuit currents that occur in the feeders. The information like fault data, transmission line data, load data, power system data, and different relay types, like Mho relay, differential relay, and impedance relay need to be considered for upcoming research. The model can be extended to other categories of relay characteristics and fault types to implement real-time relay modeling of the power system.

ACKNOWLEDGMENT

This work was supported by Moi University, Eldoret, Kenya under Africa Center of Excellence II for Phytochemical, Textile and Renewable Energy (**ACE II PTRE**) through World Bank, Prof. Paul Wambua, Prof. Simiyu Sitati and Prof. Jean Bosco Byiringiro.

REFERENCES

Aimable, N. (2020). Power blackout occured in Rwanda Electricity Grid in 2019 and later 2020. Kigali: Aimable Nsanzimana.

Akbar A., M. P. (2011). Optimal coordination of overcurrent and distance relays by a new particle swarm optimization method. International Journal of Engineering and Advanced Technology, 93–98.

Akbar, M. (2011). Optimal Coordination of Overcurrent and Distance Relays by a New Particle Swarm Optimization Method. International Journal of Engineering and Advanced Technology, 93–98.

Behera, N. (2019). Load Frequency Control of Power System. Rourkela, India: P.K Ray.

Congzhi Huang, J. L. (2017). Linear active disturbance rejection control approach for load frequency control of two-area interconnected power system. Transactions of the Institute of Measurement and Control, 1–9.

Dobson. (2007). Protection relay signals. . Mumbai: Dobson.

G. S. Thakur, A. P. (2014). 'Load frequency in Single area with tradition Ziegler-Nichols PID tuning controller. International Journal of Research in Advanced Technology.

Gerard, E. A. (2020). Total Duration of Power blackouts in Rwanda Electricity Grid Records. Kigali: Energy Utility Corporation Limited.

Gurrala, G., & Sen, I. (2010). Power system stabilizers design for interconnected power systems. IEEE Trans. on Power Systems, XXV(2), 1042–1051.

Hojo, M. O. (2005). Analysis of Load Frequency Control Dynamics Based on Multiple Synchronized Phasor Measurements. 15th PSCC (pp. 22-26). Tokushima: Hojo, M., Ohnishi, K, and Ohnishi, T.

Javad S., V. A. (2019). Optimal coordination ofovercurrent and distance relays with hybrid genetic algorithm. 10th International Conference on Environment and Electrical Engineering. Rome, Italy: Javad S.

Kundur, P. (1994). Power System Stability and Control. New York: McGraw-Hill: P. Kundur.

L. Gao, Y. W. (2016). Transient Stability Enhancement and Voltage Regulation of Power System. . L. Gao, Y.Y Wang.

Limited, E. U. (2018, 2019 and 2020). Total Blackouts in Rwanda Electricity Grid Records. Kigali: EUCL.

M. J. Hossain, H. R. (2009). Excitation Control for Large Disturbances in Power Systems with Dynamic Loads. IEEE Xplore.

M. Wadi, M. B. (2017). Comparison between Open-Ring and Closed-Ring Grids Reliability. 4th International Conference on Electrical and Electronics Engineering. Ankara: M. Wadi, M. Baysal.

Mancer N, M. B. (2015). Optimal Coordination of Directional Overcurrent Relays Using PSO. TVAC Energy Procedia (pp. 1239–1247). Hamed M.

Naresh K. Tanwani, A. P. (2014). Simulation Techniques of Electrical Power System Stability Studies Utilizing Matlab/Simulink. international journal of engineering sciences & research technology, iii(3), 1228-1240.

NEPA. (2007). Basic Protection Course P1"Training and development program. Washington: NEPA.

P. K. Modi, S. P. (2006). Stability Improvement of Power System by Decentralized Energy, Advances in Energy Research. India: P. K. Pradhan.

P. Nelson, S. M. (2017). Frequency regulation free governor mode of operation in power stations. IEEE International Conference on Computational Intelligence and Computing Research, 125–129.

Reza M., H. A. (2010). Optimal relays coordination efficient method in interconnected power systems. Journal of Electrical Engineering , 75–83.

Steinmetz, C. P. (1920). Power control and stability of electric generating stations. AIEE Trans., XXXIX(2), 1215–1287.

Tanwani, N. K. (2013). nalysis and Simulation Techniques of Electrical Power System Stability Studies. Pakistan: Naresh K. Tanwani.

W.B. (2017). frequent power outages in Rwanda. Kigali: World Bank Group.

Wang. (2010). Penetration of automation control and protection in power systems. Delhi: Wang.

Wang, L. (2016). Li Wang 2016 The Fault Causes of Overhead Lines in Distribution Network. 10.1051/ matecconf/20166102017: MATEC Web of conferences 61.

Weiss, R. (2019). Line Voltage Stability Indices Based on Precautionary MeasureApproximation in Smart Grid. Proceedings of the 11th International Conference on Innovation & Management. Kigali, Rwanda: Rwanda Energy Group.

Weiss, R. (2020). Line Voltage Stability Indices Based on Precautionary MeasureApproximation in Smart Grid. Kigali: Rwanda Energy Group.

Weiss, R. (2020). Line Voltage Stability Indices Based on Precautionary MeasureApproximation in Smart Grid. Proceedings of the 11th International Conference on Innovation & Management. Kigali, Rwanda: Rwanda Energy Group.

Z. Osman, M. Y.-D. (2006). Maximum Loadability of Power System Using Hybrid Particle Swarm Optimization. Electric Power System Research,, V(76), 485–492.

Zalostiba. (2020). blackout analysis, the dangerous overload of transmission grid in blackout analysis. Tokyo: Zalostiba.